Diagrammatic Design of Ansätze for Quantum Chemistry

Ayman El Amrani

St. John's College

A thesis submitted for the Honour School of Chemistry

Part II 2024

Pour ma mère et mon père.

Acknowledgements

Thank you Thomas Cervoni for your constant motivation and support.
Thank you David Tew and Stefano Gogioso for your patient supervision.
Thank you Razin Shaikh, Boldizsár Poór, Richie Yeung and Harny Wang for always finding the time to answer my questions.
Thank you to my friends and family for supporting me during this unconvential Master's.

Summary

A central challenge in computational quantum chemistry is the accurate simulation of fermionic systems. At the heart of these calculations lies the need to solve the Schrödinger equation to determine the many-electron wavefunction. An exact solution to this problem scales exponentially with the number of electrons. Classical computers struggle to store the increasingly large wavefunctions making this problem computationally intractable in many cases. In contrast, gate-based quantum computing presents a promising solution, offering the potential to represent electronic wavefunctions with polynomially scaling resources [1]. In other words, quantum computers are a natural tool of choice for simulating processes that are inherently quantum [2].

In the last two decades many advancements in quantum computing have been made in both hardware and software bringing us closer to being able to simulate molecular systems. Despite these advancements, we remain in the so-called Noisy Intermediate Scale Quantum (NISQ) era, characterised by challenges such as poor qubit fidelity, low qubit connectivity and limited coherence times. The NISQ era represents a transitional phase in quantum computing, where quantum devices are not yet error-corrected but are still capable of performing computations beyond the reach of classical computers. Overcoming the limitations of the NISQ era is crucial for realising the full potential of quantum computing in various fields, including quantum chemistry and materials science.

The Variational Quantum Eigensolver (VQE) algorithm is a method used to estimate the ground state energy of a molecular Hamiltonian by preparing a trial wavefunction,

calculating its energy, and optimising the wavefunction parameters classically until the energy converges to the best approximation for the ground state energy [3]. It is recognised as a leading algorithm for quantum simulation on NISQ devices due to its reduced resource requirements in terms of qubit count and coherence time [4].

This thesis extends methods developed by Richie Yeung [2] for the preparation and analysis of parametrised quantum circuits, and applies them to ansätze representing fermionic wavefunctions. We are concerned with two main questions on this theme. Firstly, can we use the ZX calculus [cite] to gain insights into the structure of the unitary product ansatz in the context of variational algorithms for quantum chemistry? Secondly, in the context of NISQ devices, can we use these insights to build better ansätze with reduced circuit depth and more efficient resources?

Contents

Chapter 1

Background

In this chapter, we will discuss the framework that we use to simulate fermionic systems on a quantum computer, as well as the notation that we will use throughout the text. Starting with Quantum Computation 1.1 and Electronic Structure Theory 1.2, we will build up to unitary coupled cluster theory and the Variational Quantum Eigensolver 1.3.

Fermionic states can generally be represented on a quantum computer in the occupation number representation (section 1.2). That is, the state of each qubit is taken to represent the occupancy of each spin orbital. By representing the fermionic creation and annhilation operators in terms of qubit operators in a way that preserves the fermionic anticommutation relations, we can express the molecular Hamiltonian in terms of qubit operations.

1.1 Quantum Computation

Introduction to Qubits

In contrast to classical computation, where bits form the basis for encoding information, quantum computation makes use of quantum bits (qubits). There are many physical implementations of qubits, however, for the purposes of this thesis, it will suffice to think of them as purely mathematical objects.

Qubits can exist as superpositions of the computational basis: the $|0\rangle$ and $|1\rangle$ states. These states are orthonormal vectors in a two-dimensional complex Hilbert space $\mathbb{C}^2$. We can depict these states on a Bloch sphere as in figure 1.1. Note that the Bloch space does not represent the complex Hilbert space itself.

More generally, we can choose any pair of orthonormal states to form our computational basis. On the bloch sphere, this corresponds to any two vectors pointing in opposite directions. One such computational basis if formed by the $|+\rangle = \frac{1}{\sqrt{2}}(|0\rangle + |1\rangle)$ and $|-\rangle = \frac{1}{\sqrt{2}}(|0\rangle - |1\rangle)$ states.

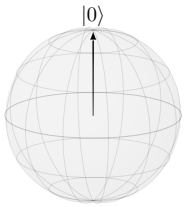

Figure 1.1: $|0\rangle$ basis state

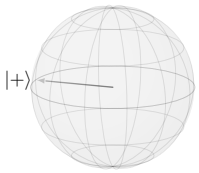

Figure 1.2: $|+\rangle$ basis state

Any qubit $|\psi\rangle$ can be represented as complex linear combination of the chosen basis, provided that the qubit state vector is normalised.

$$|\psi\rangle = \alpha\,|0\rangle + \beta\,|1\rangle \qquad |\alpha|^2 + |\beta|^2 = 1 \qquad \alpha, \beta \in \mathbb{C}$$

Multiple Qubit States

Suppose we have n qubits. By taking the Kronecker product, we can construct 2^n computational basis states.

$$|00\ldots00\rangle = |0\rangle_n \otimes |0\rangle_{n-1} \otimes \cdots \otimes |0\rangle_1 \otimes |0\rangle_0$$
$$\cdots$$
$$|11\ldots11\rangle = |1\rangle_n \otimes |1\rangle_{n-1} \otimes \cdots \otimes |1\rangle_1 \otimes |1\rangle_0$$

Figure 1.3: 2^n computational basis states.

It follows then that any complex linear combination of the computational basis states is also a valid qubit state.

$$|\psi\rangle = \alpha_{00\ldots00}\,|00\ldots00\rangle + \alpha_{00\ldots01}\,|00\ldots01\rangle + \cdots + \alpha_{11\ldots11}\,|11\ldots11\rangle$$

Whilst the Bloch sphere representation of a single qubit is incredibly useful, there is no easy generalisation of the Bloch sphere for multiple qubit states [5].

Quantum Gates

1.2 Electronic Structure Theory

Electronic Structure Problem

References: [6]

The main interest of electronic structure theory is finding approximate solutions to the eigenvalue equation of the full molecular Hamiltonian. Specifically, we seek solutions to the non-relativistic time-independent Schrödinger equation.

$$H = -\sum_{i=1}^{N} \frac{1}{2}\nabla_i^2 - \sum_{i=1}^{M} \frac{1}{2M_i}\nabla_i^2 - \sum_{i=1}^{N}\sum_{j=1}^{M} \frac{Z_j}{|r_i - R_j|} + \sum_{i=1}^{N}\sum_{j>i}^{N} \frac{1}{|r_i - r_j|} + \sum_{i=1}^{M}\sum_{j>i}^{M} \frac{Z_i Z_j}{|R_i - R_j|}$$

Figure 1.4: Full molecular Hamiltonian in atomic units, where Z_i is the charge of nucleus i and M_i is its mass relative to the mass of an electron.

The full molecular Hamiltonian, H, describes all interactions within a system of N interacting electrons and M nuclei. The first term corresponds to the kinetic energy of all electrons in the system. The second term corresponds to the total kinetic energy of all nuclei. The third term corresponds to the pairwise attractive Coulombic interactions between the N electrons and M nuclei, whilst the fourth and fifth terms correspond to all repulsive Coulombic interactions between electrons and nuclei respectively.

We are able to simplify the problem to an electronic one using the Born-Oppenheimer approximation. Motivated by the large difference in mass of electrons and nuclei, we can approximate the nuclei as stationary on the timescale of electronic motion such that the electronic wavefunction depends only parametrically on the nuclear coordinates. The full molecular wavefunction can then be expressed as an adiabatic separation as below.

$$\Phi_{\text{total}} = \psi_{\text{elec}}(\{r\};\{R\})\,\psi_{\text{nuc}}(\{R\})$$

Within this approximation, the nuclear kinetic energy term can be neglected and the nuclear repulsive term is considered to be constant. Since constants in

eigenvalue equations have no effect on the eigenfunctions and simply add to the resulting eigenvalue, we will omit this too. The resulting equation is the electronic Hamiltonian for N electrons.

$$H = -\sum_{i=1}^{N} \frac{1}{2}\nabla_i^2 - \sum_{i=1}^{N}\sum_{j=1}^{M} \frac{Z_j}{|r_i - R_j|} + \sum_{i=1}^{N}\sum_{j>i}^{N} \frac{1}{|r_i - r_j|}$$

Figure 1.5: Electronic molecular Hamiltonian in atomic units.

Throughout the remainder of this text, we will concern ourselves only with the electronic Hamiltonian, simply referring to it as the Hamiltonian, H. The solution to the eigenvalue equation involving the electronic Hamiltonian is the electronic wavefunction, which depends only parametrically on the nuclear coordinates. It is solved for fixed nuclear coordinates, such that different arrangements of nuclei yields different functions of the electronic coordinates. The total molecular energy can then be calculated by solving the electronic Schrödinger equation and including the constant repulsive nuclear term.

$$E_{\text{total}} = E_{\text{elec}} + \sum_{i=1}^{M}\sum_{j>i}^{M} \frac{Z_i Z_j}{|R_i - R_j|}$$

Many-Electron Wavefunctions

References: [6]

The many-electron wavefunction, which describes all fermions in given molecular system, must satisfy the Pauli principle. This is an independent postulate of quantum mechanics that requires the many-electron wavefunction to be antisymmetric with respect to the exchange of any two fermions.

A spatial molecular orbital is defined as a one-particle function of the position vector, spanning the whole molecule. The spatial orbitals form an orthonormal set $\{\psi_i(\mathbf{r})\}$, which if complete can be used to expand any arbitrary single-particle molecular wavefunction, that is, an arbitrary single-particle function of the position vector. In practice, only a finite set of such orbitals is available to us, spanning only

a subspace of the complete space. Hence, wavefunctions expanded using this finite set are described as being 'exact' only within the subspace that they span.

We will now introduce the spin orbitals $\{\phi_i(\mathbf{x})\}$, that is, the set of functions of the composite coordinate $\mathbf{x}$, which describes both the spin and spatial distribution of an electron. Given a set of K spatial orbitals, we can construct $2K$ spin orbitals by taking their product with the orthonormal spin functions $\alpha(\omega)$ and $\beta(\omega)$. Whilst the Hamiltonian operator makes no reference to spin, it is a necessary component when constructing many-electron wavefunctions in order to correctly antisymmetrise the wavefunction with respect to fermion exchange. Constructing the antisymmetric many-electron wavefunction from a finite set of spin orbitals amounts to taking the appropriate linear combinations of symmetric products of N spin orbitals known as Hatree products.

$$\psi_{1,2}(\mathbf{x_1}, \mathbf{x_2}) = \phi_i(\mathbf{x_1})\phi_j(\mathbf{x_2}) \qquad \psi_{2,1}(\mathbf{x_2}, \mathbf{x_1}) = \phi_i(\mathbf{x_2})\phi_j(\mathbf{x_1})$$
$$\Psi_{1,2}(\mathbf{x_1}, \mathbf{x_2}) = \frac{1}{\sqrt{2}}\left[\psi_{1,2}(\mathbf{x_1}, \mathbf{x_2}) - \psi_{2,1}(\mathbf{x_2}, \mathbf{x_1})\right]$$

Figure 1.6: Symmetric Hartree products $\psi_{1,2}(\mathbf{x_1}$ and $\mathbf{x_2})$, $\psi_{2,1}(\mathbf{x_2}, \mathbf{x_1})$, and their antisymmetric linear combination $\Psi_{1,2}(\mathbf{x_1}, \mathbf{x_2})$.

A general procedure for this is achieved by constructing a Slater determinant from the finite set of spin orbitals, where each row relates to the electron coordinate $\mathbf{x_n}$ and each column corresponds to a particular spin orbital ϕ_i.

$$\psi(\mathbf{x}_1, \mathbf{x}_2) = \frac{1}{\sqrt{N!}} \begin{vmatrix} \phi_i(\mathbf{x}_1) & \phi_j(\mathbf{x}_1) & \dots & \phi_k(\mathbf{x}_1) \\ \phi_i(\mathbf{x}_2) & \phi_j(\mathbf{x}_2) & \dots & \phi_k(\mathbf{x}_2) \\ \vdots & \vdots & & \vdots \\ \phi_i(\mathbf{x}_N) & \phi_j(\mathbf{x}_N) & \dots & \phi_k(\mathbf{x}_N) \end{vmatrix}$$

Figure 1.7: Slater determinant representing an antisymmetrised N-electron wavefunction.

Since exchanging any two rows or columns of a determinant changes its sign, Slater determinants satisfy the Pauli principle by definition. Slater determinants

constructed from orthonormal spin orbitals are themselves normalised and N electron Slater determinants constructed from different orthonormal spin orbitals are orthogonal to one another [6].

By constructing Slater determinants and antisymmetrising the many-electron wavefunction to meet the requirements of the Pauli principle, we have incorporated exchange correlation, in that, the motion of two electrons with parallel spins is now correlated.

The Hartree-Fock method yields a set of orthonormal spin orbitals, which when used to construct a single Slater determinant, gives the best variational approximation to the ground state of a system [6]. By treating electron-electron repulsion in an average way, the Hartree-Fock approximation allows us to iteratively solve the Hartree-Fock equation for spin orbitals until they become the same as the eigenfunctions of the Fock operator. This is known as the Self-Consistent Field (SCF) method and is an elegant starting point for finding approximate solutions to the many-electron wavefunction.

$$\left[-\frac{1}{2}\nabla^2 - \sum_{A=1}^{M}\frac{Z_A}{r_{i_A}} + \boldsymbol{\nu}^{\mathrm{HF}}(i)\right]\phi_i(\mathbf{x}_i) = \varepsilon\phi_i(\mathbf{x}_i)$$

Figure 1.8: Hartree-Fock equation.

For an N electron system, and given a set of $2K$ Hartree-Fock spin orbitals, where $2K > N$, there exist many different single Slater determinants. The Hartree-Fock groundstate being one of these. The remainder are excited Slater determinants, recalling that all of these must be orthogonal to one-another. By treating the Hartree-Fock ground state as a reference state, we can describe the excited states relative to the reference state, as single, double, ..., N-tuple excited states [6].

Second Quantisation

References: [7], [8]

1. Background

In second quantisation, both observables and states (by acting on the vacuum state) are represented by operators, namely the creation and annhilation operators [7]. In contrast to the standard formulation of quantum mechanics, operators in second quantisation incorporate the relevant Bose or Fermi statistics each time they act on a state, circumventing the need to keep track of symmetrised or antisymmetrised products of single-particle wavefunctions [8]. Put differently, the antisymmetry of an electronic wavefunction simply follows from the algebra of the creation and annhilation operators [7], which greatly simplifies the discussion of systems of many identical interacting fermions [8].

The Fock space is a linear abstract vector space spanned by N orthonormal occupation number vectors [7], each representing a single Slater determinant. Hence, given a basis of N spin orbitals we can construct 2^N single Slater determinants, each corresponding to a single occupation number vector in the full Fock space.

The occupation number vector for fermionic systems is succinctly denoted in Dirac notation as below, where the occupation number f_j is 1 if spin orbital j is occupied, and 0 if spin orbital j is unnoccupied.

$$|\psi\rangle = |f_{n-1}\ f_{n-2} \dots f_1\ f_0\rangle \qquad \text{where } f_j \in 0, 1$$

Whilst there is a one-to-one mapping between Slater determinants with canonically ordered spin orbitals and the occupation number vectors in the Fock space, it is important to distinguish between the two since, unlike the Slater determinants, the occupation number vectors have no spatial structure and are simply vectors in an abstract vector space. [7].

Creation and Annhilation Operators

References: [7]

Operators in second quantisation are constructed from the creation and annhilation operators $a_j^\dagger$ and a_j, where the subscripts i and j denote the spin orbital. $a_j^\dagger$ and a_j are one another's Hermitian adjoints, and are not self-adjoint [7].

Taking the excitation of an electron from spin orbital 0 to spin orbital 1 as an example, we can construct the following excitation operator.

$$a_1^\dagger \, a_0 \, |0 \ldots 01\rangle = |0 \ldots 10\rangle$$

show ladder operators acting on opposite states

Due to the fermionic exchange anti-symmetry imposed by the Pauli principle, the action of the creation and annhilation operators introduces a phase to the state that depends on the parity of the spin orbitals preceding the target spin orbital.

$$a_j^\dagger \, |f_{n-1} \ldots f_{j+1}, \; 0, \; f_{j-1} \ldots f_0\rangle = (-1)^{\sum_{s=0}^{j-1} f_s} \, |f_{n-1} \ldots f_{j+1}, \; 1, \; f_{j-1} \ldots f_0\rangle$$
$$a_j \, |f_{n-1} \ldots f_{j+1}, \; 1, \; f_{j-1} \ldots f_0\rangle = (-1)^{\sum_{s=0}^{j-1} f_s} \, |f_{n-1} \ldots f_{j+1}, \; 0, \; f_{j-1} \ldots f_0\rangle$$

In second quantisation, this exchange anti-symmetry requirement is accounted for by the anti-commutation relations of the creation and annhilation operators.

$$\{\hat{a}_j, \hat{a}_k\} = 0 \qquad \{\hat{a}_j^\dagger, \hat{a}_k^\dagger\} = 0 \qquad \{\hat{a}_j, \hat{a}_k^\dagger\} = \delta_{jk}\hat{1}$$

Figure 1.9: Anti-commutation relations of fermionic creation and annhilation operators.

The phase factor required for the second quantised representation to be consistent with the first quantised representation is automatically kept track of by the anticommutation relations of the creation and annhilation operators [7].

Hamiltonian in Second Quantisation

The Hamiltonian in second quantisation is constructed from creation and annhilation operators as follows.

$$\hat{H} = \sum_{ij} h_{ij} a_i^\dagger a_j + \frac{1}{2} \sum_{ijkl} h_{ijkl} a_i^\dagger a_j^\dagger a_k a_l + h_{\mathrm{Nu}}$$

Where the one-body matrix element h_{ij} corresponds to the kinetic energy of an electron and its interaction energy with the nuclei.

$$h_{ij} = \int_{-\infty}^{\infty} \psi_{i(x_1)}^* \left(-\frac{1}{2}\nabla^2 + \hat{V}_{(x_1)} \right) \psi_{j(x_1)} \; d^3x_1$$

1. Background

The two-body matrix element h_{ijkl} corresponds to the repulsive interaction between electrons i and j.

$$h_{ijkl} = \int_{-\infty}^{\infty} \int_{-\infty}^{\infty} \psi^*_{i(x_1)} \psi^*_{j(x_2)} \left(\frac{1}{|x_1 - x_2|} \right) \psi_{k(x_2)} \psi_{l(x_1)} \; d^3x_1 d^3x_2$$

h_{Nu} is a constant corresponding to the repulsive interaction between nuclei. These matrix elements are computed classically, allowing us to simulate only the inherently quantum aspects of the problem on a quantum computer.

1.3 Variational Quantum Eigensolver

References: [9], [3], [10]

Fermion-Qubit Encodings

References: [11]

In order to represent the fermionic wavefunction on a quantum computer, we must first create a mapping betweent the fermionic state vector and the qubit state vector. There are a number of fermion-qubit encodings used today including the Jordan-Wigner transformation, Bravyi-Kitaev transformation and the Parity mapping. Whilst the Bravyi-Kitaev transformation and Parity mappings can more efficiently encode the fermionic wavefunction in some ways, we will only consider the Jordan-Wigner transformation for the remainder of this text as its simplicity provides us with a more intuitive picture of the computation.

The form of the occupation number representation vector and the qubit statevector suggests the following identification between electronic states and qubit states.

$$|f_{n-1}\dots f_0\rangle \quad \rightarrow \quad |q_{n-1}\dots q_0\rangle$$

That is, we allow each qubit to store the occupation number of a given spin-orbital. Hence, in order to actually simulate a Hamiltonian we must map the fermionic creation and annhilation operators onto qubit operators, and these operators must behave in the same way as their fermionic analogues.

$$\hat{Q}^+|0\rangle = |1\rangle \qquad \hat{Q}^+|1\rangle = 0 \qquad \hat{Q}|1\rangle = |0\rangle \qquad \hat{Q}|0\rangle = 0$$

The qubit operators must also preserve the fermionic anti-commutation relations in order to satisfy the Pauli antisymmetry requirement.

$$\{\hat{Q}_j, \hat{Q}_k\} = 0 \qquad \{\hat{Q}_j^\dagger, \hat{Q}_k^\dagger\} = 0 \qquad \{\hat{Q}_j, \hat{Q}_k^\dagger\} = \delta_{jk}$$

One such qubit encoding is known as the Jordan-Wigner transformation. It expresses the fermionic creation and annhilation operators as a linear combination of the

Pauli matrices.

$$\hat{Q}^{+} = |1\rangle\langle 0| = \frac{1}{2}(X - iY) \qquad \hat{Q} = |0\rangle\langle 1| = \frac{1}{2}(X + iY)$$

When dealing with **multiple-qubits**, we must also account for the occupation parity of the qubits preceding the target qubit j.

$$a_j^{\dagger}\,|f_{n-1}\dots f_{j+1},\ 0,\ f_{j-1}\dots f_0\rangle = (-1)^{\sum_{s=0}^{j-1} f_s}\,|f_{n-1}\dots f_{j+1},\ 1,\ f_{j-1}\dots f_0\rangle$$

We do this by introducing a string of Pauli Z operators that computes the parity of the qubits preceding the target qubit.

$$\hat{a}_j^{+} = \frac{1}{2}(X - iY)\prod_{k=1}^{j-1} Z_k \qquad \hat{a}_j = \frac{1}{2}(X + iY)\prod_{k=1}^{j-1} Z_k$$

Where $\prod$ is the tensor product.

A more compact notation is,

$$\hat{a}_j^{+} = \frac{1}{2}(X - iY)\otimes Z_{j-1}^{\rightarrow} \qquad \hat{a}_j = \frac{1}{2}(X + iY)\otimes Z_{j-1}^{\rightarrow}$$

Where $Z_i^{\rightarrow}$ is the parity operator with eigenvalues ± 1, and ensures the correct phase is added to the qubit state vector.

$$Z_i^{\rightarrow} = Z_i \otimes Z_{i-1} \otimes \cdots \otimes Z_0$$

For instance, the creation operator $a_3^{\dagger}$ maps to the following Pauli string,

$$\hat{a}_3^{\dagger} = \frac{1}{2}(X_3 - iY_3)\otimes Z_2 \otimes Z_1 \otimes Z_0$$
$$\hat{a}_3^{\dagger} = \frac{1}{2}(X_3 \otimes Z_2 \otimes Z_1 \otimes Z_0) - \frac{1}{2}i(Y_3 \otimes Z_2 \otimes Z_1 \otimes Z_0)$$

Usually we drop the subscript specifying the orbital acted on.

Unitary Coupled Cluster

Whilst unitary coupled cluster theory was proposed in X, interest in its applications has been minimal due to the inability of classical computers to efficiently evaluate its equations. As suggested by Peruzzo et al [12], the UCC formulation of a

wavefunction can be efficiently implemented on a quantum computer using quantum gates.

Unitary coupled cluster theory allows us to represent an arbitrary state $|\psi\rangle$ using the following exponential ansatz.

$$|\psi\rangle = e^{\hat{T}(\theta)-\hat{T}^{\dagger}(\theta)}\,|\psi_0\rangle$$

Where $|\psi_0\rangle$ is a single reference Slater determinant, usually the Hartree-Fock groundstate obtained via the self-consistent field method. The exponential operator $U(\theta) = e^{\hat{T}(\theta)-\hat{T}^{\dagger}(\theta)}$ is unitary since its exponent $\hat{T}(\theta) - \hat{T}^{\dagger}(\theta)$ is anti-Hermitian.

The excitation operators are given by

$$\hat{T}(\theta) - \hat{T}^{\dagger}(\theta) = \sum_{i,a} \theta_i^a (a_i^{\dagger} a_a - a_a^{\dagger} a_i) + \sum_{i,j,a,b} \theta_{ij}^{ab} (a_i^{\dagger} a_j^{\dagger} a_a a_b - a_a^{\dagger} a_b^{\dagger} a_i a_j) + \ldots$$

Where i, j indexes occupied spin orbitals and a, b indexes virtual, or unoccupied, spin orbitals. The resulting unitary operator $U(\theta)$ cannot be directly implemented on a quantum computer since the terms of the excitation operator do not commute. Instead, we must invoke the Trotter formula to approximate the unitary.

$$e^{A+B} = (e^{A}\, e^{B})^{\rho}$$

Taking a single Trotter step $\rho = 1$, we obtained the disentangled UCC

$$U_{t1}(\theta) = \prod_m e^{\theta_m(\tau_m - \tau_m^{\dagger})} \tag{1.1}$$

Where m indexes all possible excitations. It has been shown in [13] that the disentangled UCC can exactly parametrise any state.

"In practice, the excitations are truncated to only include single and double excitations. This UCCSD ansatz has been popular in the VQE literature and is often the benchmark for more cost effective methods." [10].

1. Background

"Only UCCSD excitation operators which conserve spin were used for ansatz construction. Ansatze generated in this manner preserve the spin symmetry of the spin reference" [10]

—

In this chapter we introduce we introduce Unitary Coupled Cluster theory which will serve as the basis for the Variational Quantum Eigensolver algorithm introduced in chapter XXX. In particular, we are interested in developing the Unitary-Product State which will serve as a variational ansatz.

One notable advantage of the VQE algorithm is its ability to be run on any quantum architecture, moreover, we can leverage architecture requirements when designing the variational ansatz. [3].

"Even in the event that some error correction is required to exceed current computational capabilities, this same robustness may translate to requiring minimal error cor- rection resources when compared with other algorithms." [3]

We begin by...

Within the traditional coupled-cluster framework, the ground electronic state is prepared by applying the CC operator to a reference state (usually Hartree-Fock).

$$|\psi\rangle = e^{\hat{T}} |\phi_0\rangle$$

Where $\hat{T}$ is the cluster excitation operator.

Quantum gates, however, must be unitary operators, so instead, we work within the UCC framework.

$$|\psi\rangle = e^{\hat{T}} |\phi_0\rangle$$

Where $\hat{T}$ is now an **anti-Hermitian** operator, and $e^{\hat{T}}$ is unitary.

1. Background

In general, we can prepare exact electronic states by applying a sequence of k parametrised unitary operators to our reference state.

$$|\psi\rangle = \prod_{i}^{k} U_i(\theta_i) \, |\phi_0\rangle$$

Where $U_i(\theta_i)$ is a parametrised unitary operator

The parameters θ_i are then optimised to find the ground state energy.

General fermionic single and double excitation operators are defined as,

$$a_q^\dagger a_p \text{ and } a_r^\dagger a_s^\dagger a_q a_p$$

Exciting one electron from p to q, and two electrons from p, q to r, s respectively.

Taking a linear combination of these, we obtain **anti-Hermitian** fermionic single and double excitation operators.

$$\hat{\kappa}_p^q = a_q^\dagger a_p - a_p^\dagger a_q$$
$$\hat{\kappa}_{pq}^{rs} = a_r^\dagger a_s^\dagger a_q a_p - a_p^\dagger a_q^\dagger a_s a_r$$

Such that upon exponentiating, we obtain **unitary** operators.

$$U_p^q = e^{\hat{\kappa}_p^q} \qquad U_{pq}^{rs} = e^{\hat{\kappa}_{pq}^{rs}}$$

Variational Quantum Eigensolver

Recalling the Jordan-Wigner encoding for the creation and annhilation operators,

$$\hat{a}_j^+ = \frac{1}{2}(X - iY) \otimes Z_{j-1}^{\rightarrow} \qquad \hat{a}_j = \frac{1}{2}(X + iY) \otimes Z_{j-1}^{\rightarrow}$$

1. Background

The anti-Hermitian fermionic single and double excitation operators κ_p^q and κ_{pq}^{rs}

$$F_p^q = \frac{i}{2}(Y_pX_q - X_pY_q)\prod_{k=p+1}^{q-1} Z_k$$

$$F_{pq}^{rs} = \frac{i}{8}(X_pX_qY_sX_r + Y_pX_qY_sY_r + X_pY_qY_sY_r + X_pX_qX_sY_r - Y_pX_qX_sX_r - X_pY_qX_sX_r - Y_pY_qY_sX_r - Y_pY_qX_sY_r)\prod_{k=p+1}^{q-1} Z_k \prod_{l=r+1}^{s-1} Z_l$$

Multiplying by θ and exponentiating yields the parametrised unitary qubit operators,

$$U_p^q(\theta) = \exp\left(i\frac{\theta}{2}(Y_pX_q - X_pY_q)\prod_{k=p+1}^{q-1} Z_k\right)$$

$$U_{pq}^{rs}(\theta) = \exp\left(i\frac{\theta}{8}(X_pX_qY_sX_r + \cdots - Y_pY_qY_sX_r - Y_pY_qX_sY_r)\prod_{k=p+1}^{q-1} Z_k \prod_{l=r+1}^{s-1} Z_l\right)$$

To summarise, we constructed anti-Hermitian single and double excitation operators from a linear combination of fermionic excitation operators,

$$\hat{\kappa}_p^q = a_q^\dagger a_p - a_p^\dagger a_q \qquad \hat{\kappa}_{pq}^{rs} = a_r^\dagger a_s^\dagger a_q a_p - a_p^\dagger a_q^\dagger a_s a_r$$

We then mapped these to qubit operators using the Jordan-Wigner transformation,

$$\hat{\kappa}_p^q \xrightarrow{\text{JW}} F_p^q \qquad\qquad \hat{\kappa}_{pq}^{rs} \xrightarrow{\text{JW}} F_{pq}^{rs}$$

And finally, we exponentiated to yield the parametrised unitary qubit operators.

$$U_p^q(\theta) = e^{\theta_p^q F_p^q} \qquad U_{pq}^{rs}(\theta) = e^{\theta_{pq}^{rs} F_{pq}^{rs}}$$

Let's look again at the parametrised single-body unitary operator,

$$U_p^q(\theta) = \exp\left(i\frac{\theta}{2}(Y_pX_q - X_pY_q)\prod_{k=p+1}^{q-1} Z_k\right)$$

$$U_p^q(\theta) = \left(\exp\left[i\frac{\theta}{2}Y_pX_q\prod_{k=p+1}^{q-1} Z_k\right]\right)\left(\exp\left[-i\frac{\theta}{2}X_pY_q\prod_{k=p+1}^{q-1} Z_k\right]\right)$$

The first exponential term can be implemented by the following phase gadget.

$$\exp\left(i\frac{\theta}{2}Y_pX_q\prod_{k=p+1}^{q-1}Z_k\right)$$

Left CNOT ladder construction calculates the parity of the qubit state, and applies a rotation in the Z basis if the parity is odd.

Whilst the second exponential term can be implemented by the phase gadget.

$$\exp\left(-i\frac{\theta}{2}X_pY_q\prod_{k=p+1}^{q-1}Z_k\right)$$

Together, they constitute the single-body unitary excitation operator $U_p^q(\theta)$

By defining the ordering of spin-orbitals such that adjacent spin-orbitals share the same spatial orbital, adjacent single-body operators commute.

$$\left[\hat{\kappa}_p^q, \hat{\kappa}_{p+1}^{q+1}\right] = 0$$

The same is therefore true for the resulting qubit operators,

$$\left[F_p^q, F_{p+1}^{q+1}\right] = 0$$
$$p, q \in \text{even} \qquad p+1, q+1 \in \text{odd}$$

This allows us to define the parametrised unitary qubit operators in terms of spin-adapted excitation operators.

$$U_p^q(\theta) = \exp\left[\theta\left(F_p^q + F_{p+1}^{q+1}\right)\right]$$

In other words, since F_p^q and F_{p+1}^{q+1} commute, we can think of them as a single operator with a single parameter.

Chapter 2

ZX Calculus

The ZX calculus is a diagrammatic language for reasoning about quantum processes that has seen a large increase in applications over the past 10 years. It provides a novel perspective on quantum computation and quantum mechanics.

2.1 Generators

By sequentially or horizontally composing the *Z Spider* (green) and *X Spider* (red) generators, we can construct undirected multigraphs known as ZX diagrams [14]. That is, graphs that allow multiple edges between vertices. Since *only connectivity matters* in the ZX calculus, a valid ZX diagram can be deformed as seen fit, provided that the order of inputs and outputs is preserved.

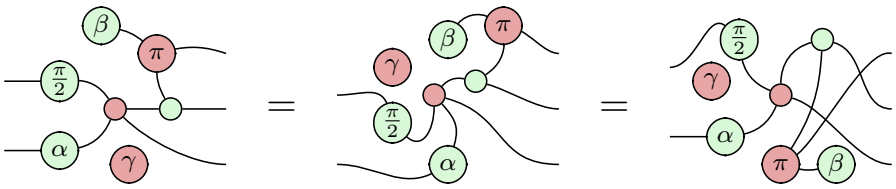

Figure 2.1: Three equivalent ZX diagrams (*only connectivity matters*).

Z Spiders are defined with respect to the Z eigenbasis such that a Z Spider with n inputs and m outputs has the following interpretation as a linear map. Note that in this text, we will interpret the flow of time from left to right.

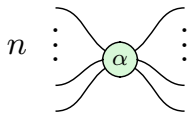

$$= |0\rangle^{\otimes m} \langle 0|^{\otimes n} + e^{i\alpha} |1\rangle^{\otimes m} \langle 1|^{\otimes n}$$

Figure 2.2: Interpretation of Z Spider as a linear map.

Similarly, X Spiders, which are defined with respect to the X eigenbasis, are interpreted as the following linear map.

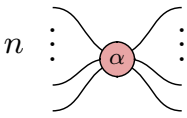

$$= |+\rangle^{\otimes m} \langle +|^{\otimes n} + e^{i\alpha} |-\rangle^{\otimes m} \langle -|^{\otimes n}$$

Figure 2.3: Interpretation of X Spider as a linear map.

We can recover the $|0\rangle$ eigenstate using an X Spider that has a phase of zero, or the $|1\rangle$ eigenstate using an X Spider that has a phase of π.

$$= |+\rangle + |-\rangle = \sqrt{2}\,|0\rangle$$

Figure 2.4: $|0\rangle$ eigenstate

$$= |+\rangle - |-\rangle = \sqrt{2}\,|1\rangle$$

Figure 2.5: $|1\rangle$ eigenstate

Likewise, we have the $|+\rangle$ and $|-\rangle$ basis states from the corresponding Z Spider

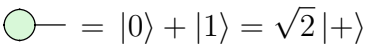

Figure 2.6: $|+\rangle$ eigenstate

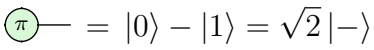

Figure 2.7: $|-\rangle$ eigenstate

Whilst we obtain the correct states, we obtain the wrong scalar factor. For the remainder of this thesis, we will ignore global non-zero scalar factors. Hence, equal signs should be interpreted as 'equal up to a global phase'.

Single qubit rotations in the Z basis are represented by a Z Spider with a single input and a single output. Arbitrary rotations in the X basis are represented by the corresponding X spider. We can view these as rotations of the Bloch sphere.

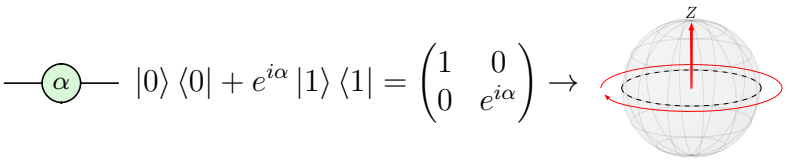

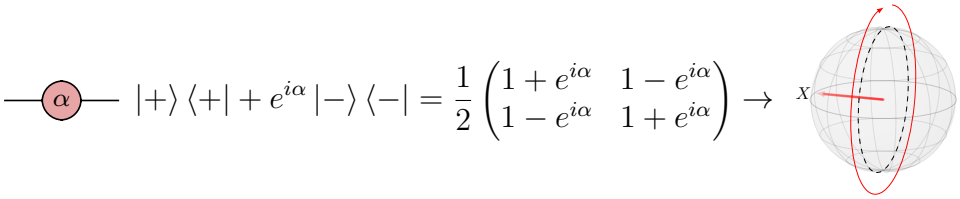

Figure 2.8: Arbitrary single qubit rotations in the Z and X bases.

We can recover the Pauli Z and Pauli X matrices by setting the angle $\alpha = \pi$.

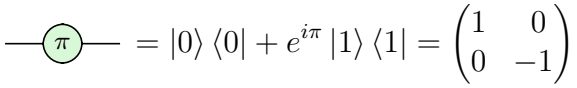

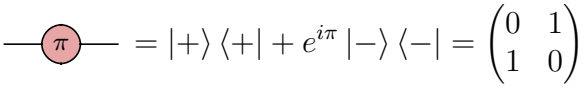

Figure 2.9: Pauli Z and X gates in the ZX calculus.

Composition

To calculate the matrix of a ZX diagram consisting of sequentially composed spiders, we take the matrix product. Note that the order of operation of matrix

multiplication is the reverse as in the ZX diagram as we have defined it.

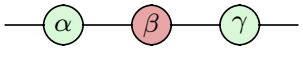

$$= \begin{pmatrix} 1 & 0 \\ 0 & e^{i\gamma} \end{pmatrix} \begin{pmatrix} 1+e^{i\beta} & 1-e^{i\beta} \\ 1-e^{i\beta} & 1+e^{i\beta} \end{pmatrix} \begin{pmatrix} 1 & 0 \\ 0 & e^{i\alpha} \end{pmatrix}$$

Alternatively, we could have chosen to compose the spiders in parallel, resulting in the tensor product.

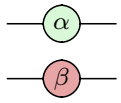

$$= \begin{pmatrix} 1 & 0 \\ 0 & e^{i\alpha} \end{pmatrix} \otimes \begin{pmatrix} 1+e^{i\beta} & 1-e^{i\beta} \\ 1-e^{i\beta} & 1+e^{i\beta} \end{pmatrix}$$

The CNOT gate in the ZX calculus is represented by a Z spider (control qubit) and an X spider (target qubit). We can arbitrarily deform the diagram and decompose it into matrix and tensor products as follows.

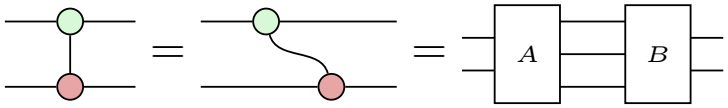

We can calculate matrix A, consisting of a single-input and two-output Z Spider (4×2 matrix) and an empty wire (identity matrix), by taking the tensor product.

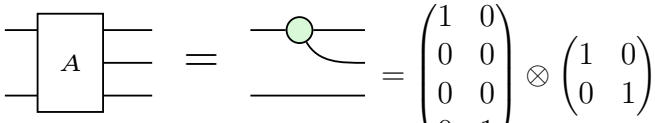

$$= \begin{pmatrix} 1 & 0 \\ 0 & 0 \\ 0 & 0 \\ 0 & 1 \end{pmatrix} \otimes \begin{pmatrix} 1 & 0 \\ 0 & 1 \end{pmatrix}$$

Similarly, to calculate the matrix B, we take the following tensor product.

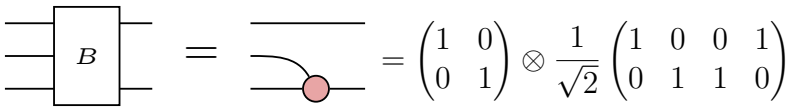

$$= \begin{pmatrix} 1 & 0 \\ 0 & 1 \end{pmatrix} \otimes \frac{1}{\sqrt{2}} \begin{pmatrix} 1 & 0 & 0 & 1 \\ 0 & 1 & 1 & 0 \end{pmatrix}$$

We can then calculate the CNOT matrix by taking the matrix product of matrix A and matrix B as follows.

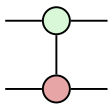

$$= \left[\begin{pmatrix} 1 & 0 \\ 0 & 1 \end{pmatrix} \otimes \frac{1}{\sqrt{2}} \begin{pmatrix} 1 & 0 & 0 & 1 \\ 0 & 1 & 1 & 0 \end{pmatrix} \right] \left[\begin{pmatrix} 1 & 0 \\ 0 & 0 \\ 0 & 0 \\ 0 & 1 \end{pmatrix} \otimes \begin{pmatrix} 1 & 0 \\ 0 & 1 \end{pmatrix} \right] \simeq \begin{pmatrix} 1 & 0 & 0 & 0 \\ 0 & 1 & 0 & 0 \\ 0 & 0 & 0 & 1 \\ 0 & 0 & 1 & 0 \end{pmatrix}$$

Had we chosen to make the first qubit the target and the second qubit the control, we would have obtained the following.

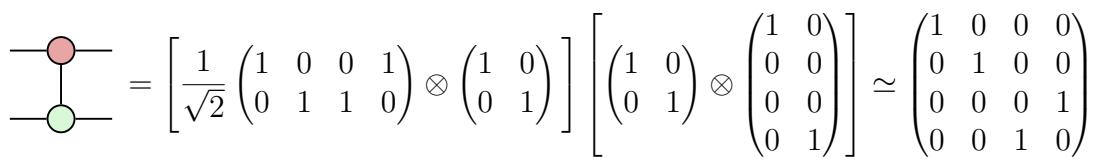

Since *only connectivity matters*, we could have equivalently calculated the matrix of the CNOT gate by deforming the diagram as follows.

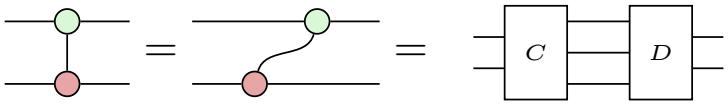

Hadamard Generator

All quantum gates are unitary transformations. Therefore, up to a global phase, an arbitrary single qubit rotation U can be viewed as a rotation of the Bloch sphere about some axis. We can decompose the unitary U using Euler angles to represent the rotation as three successive rotations [14].

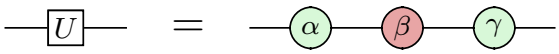

Figure 2.10: Arbitrary single-qubit rotation.

Recall that the Hadamard gate H switches between the $|0\rangle/|1\rangle$ and $|+\rangle/|-\rangle$ bases. That is, it corresponds to a rotation of the Bloch sphere π radians about the line bisecting the Z and X axes. By choosing $\alpha = \beta = \gamma = \frac{\pi}{2}$, we obtain the Hadamard gate up to a global phase of $e^{-i\frac{\pi}{4}}$. We define the Hadamard generator below.

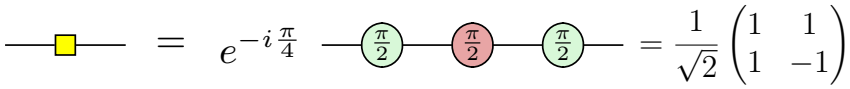

Figure 2.11: Hadamard generator in the ZX calculus.

There are many equivalent ways of decomposing the Hadamard gate using Euler angles. Note that the rightmost representations need no scalar corrections.

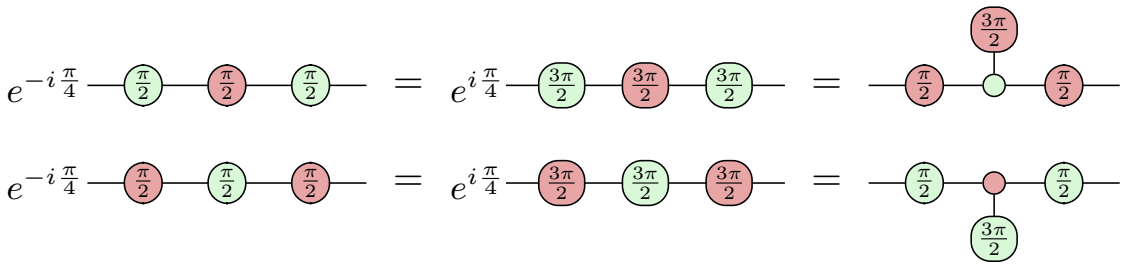

Figure 2.12: Equivalent definitions of the Hadamard generator.

Conjugate, Transpose and Adjoint

We can find the transpose of a ZX diagram by turning all of its inputs into outputs and all of its outputs into inputs whilst preserving the order of their wires.

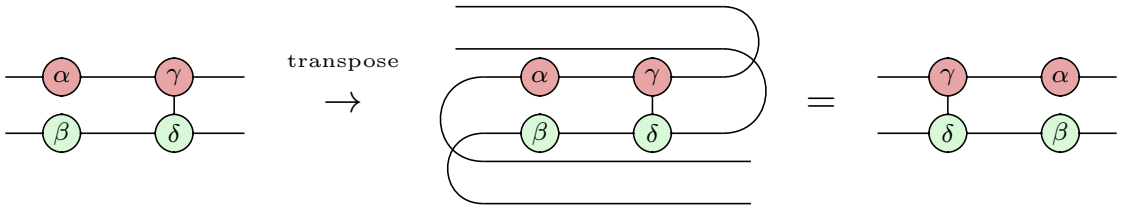

We can find the conjugate of a ZX diagram by simply negating the phases of all spiders in the diagram, $\alpha \to -\alpha,\ \beta \to -\beta, \ldots$.

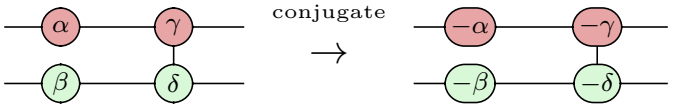

It is then a simple matter to find the Hermitian adjoint of a ZX diagram by first finding its conjugate, then its transpose.

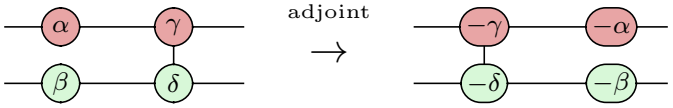

2.2 Rewrite Rules

This section introduces the various rewrite rules that come equipped with the ZX calculus. These rules extend the ZX calculus from notation into a language.

Spider Fusion

The most fundamental rule of the ZX calculus is the *spider fusion* rule [14]. It states that two spiders connected by one or more wires fuse if they are the same colour. It is the generalisation of adding the phases of successive rotations of the Bloch sphere. Since we interpret the phases α and β as $e^{i\alpha}$ and $e^{i\beta}$, it follows that the phase $\alpha + \beta$ is modulo 2π.

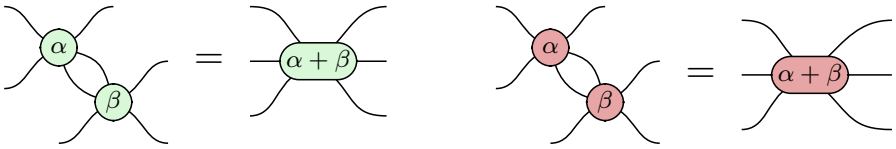

Figure 2.13: Spider fusion rule for Z spiders (left) and X spiders (right).

We can use this rule to identify commutation relations. For instance, Z rotations commute through CNOT controls and X rotations commute through CNOT targets.

Identity Removal

The *identity removal* rule states that any two-legged spider with no phase ($\alpha = 0$) is equivalent to an empty wire since a rotation by 0 radians is the same as no rotation.

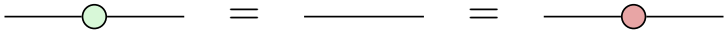

Figure 2.14: Identity removal rule.

Combining this with the spider fusion rule (2.2), we see that two successive rotations with opposite phases is equivalent to an empty wire.

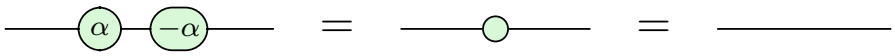

π Copy Rule

The π *copy* rule concerns itself with the interactions of the Pauli Z and X gates with spiders. It states that when a Pauli Z or Pauli X gate is pushed through a spider of the opposite colour, it copies through the spider and flips its phase.

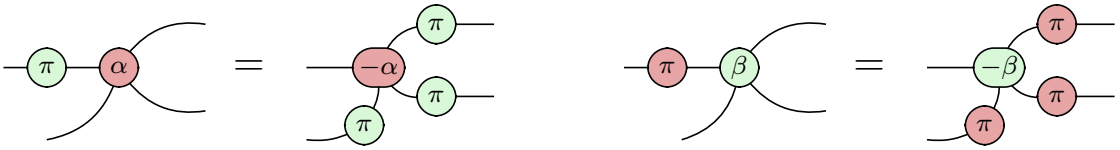

Figure 2.15: π copy rule for Z and and X spiders.

State Copy Rule

A similar rule derived from the π copy rule (2.2), is the *state copy* rule. It states that the $|0\rangle$ state (phaseless X spider) and the $|1\rangle$ state (X spider with phase π) interact with Z spiders as follows. The same rule holds for the colour-flipped counterparts.

Figure 2.16: State copy rule for the X eigenstates.

Bialgebra Rule

Unlike the previous rules we have introduced, the *bialgebra rule* takes some time to understand intuitively. It is nethertheless important in many derivations. We can represent the eigenstates of the X and Z operators by introducing the boolean variable $a \in \{0, 1\}$ as follows.

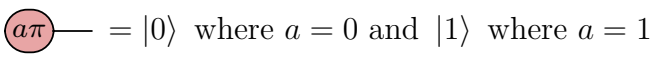

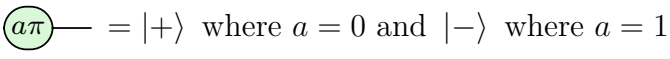

Using the spider fusion rule (2.2), we are able to show that an X spider with two inputs and one output behaves like the classical XOR gate when applied to the $|0\rangle$ and $|1\rangle$ states. Using the state copy rule (2.2), we are able to show that a Z spider with one input and two outputs behaves like the classical COPY gate.

Figure 2.17: X spider as a XOR gate (left) and Z spider as a COPY gate (right).

Let us now consider the natural commutation relation of the classical XOR and COPY gates. It is clear that XORing two bits then copying them is the same as copying the same two bits, then XORing them. Using this relation as motivation, we define the *bialgebra* rule as follows.

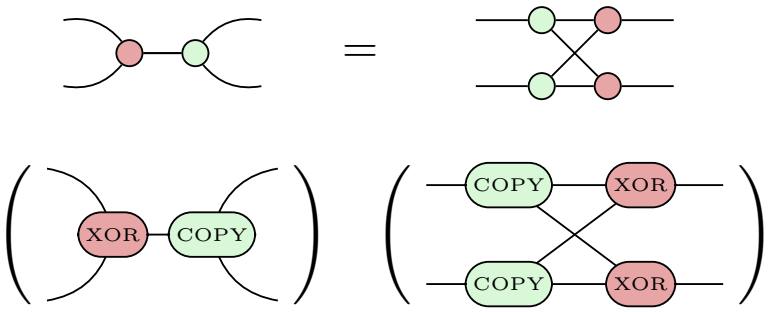

Figure 2.18: The bialgebra rule (top) and its classical motivation (bottom).

The bialgebra rule is then the quantum generalisation of the XOR-COPY commutation relation. It holds for all states, not just the computational basis states.

Hopf Rule

Finally, we have the Hopf rule, which states that we can remove the wires connecting an X spider and a Z spider when the number of connections between them is two. Like with the bialgebra rule (2.2), we can take motivation from the behaviour of the classical XOR and COPY gates, since COPYing two bits then XORing them always yields 0.

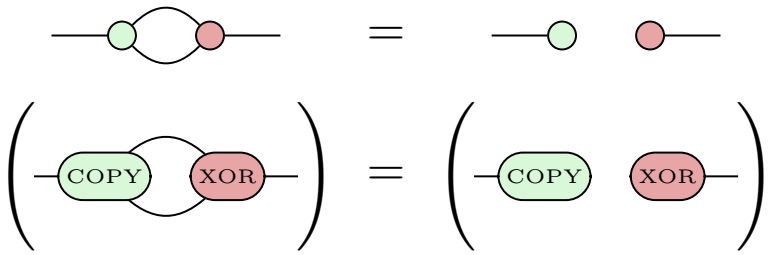

Figure 2.19: The Hopf rule (top) and its classical motivation (bottom).

Chapter 3

Pauli Gadgets

3.1 Phase Gadgets

1. zx representation
2. algebraic structure
3. relation to chemistry
4. phase gadget decomposition / ladder / bricklayering

3.2 Pauli Gadgets

$$C \in \text{Clifford} \qquad P \in \text{Pauli}$$

$$\text{prove: } Ce^{P}C^{\dagger} = e^{CPC^{\dagger}}$$

$$CP^{n}C^{\dagger} = (CPC^{\dagger})^{n}$$

$$Ce^{P}C^{\dagger} = C\sum_{n=0}^{\infty}\left(\frac{P^{n}}{n!}\right)C^{\dagger} = \sum_{n=0}^{\infty}\frac{CP^{n}C^{\dagger}}{n!} = \sum_{n=0}^{\infty}\frac{(CPC^{\dagger})^{n}}{n!}$$

3.3 Commutation Relations

Chapter 4

ZxFermion Software

ZxFermion is a Python package built on top of PyZX [15] designed for the manipulation and visualisation of circuits of Pauli gadgets. With built-in Clifford tableau logic using Stim [16], ZxFermion allows users to quickly implement proofs and test ideas.

VQE algorithms used in quantum chemistry often utilise the UCC framework in which excitation operators have a natural representation as Pauli gadgets. ZxFermion provides a comprehensive toolset designed to be used in a Jupyter notebook environment. Export functionality can be used to generated research paper quality diagrams.

4.1 Creating Gadgets

4.2 Creating Circuits

4.3 Stabiliser Circuits

Chapter 5

Commuting Excitation Operators

5.1 Operator Commutations

Chapter 6

Controlled Rotations

6.1 Singly-Controlled Rotations

Singly-controlled Z rotation.

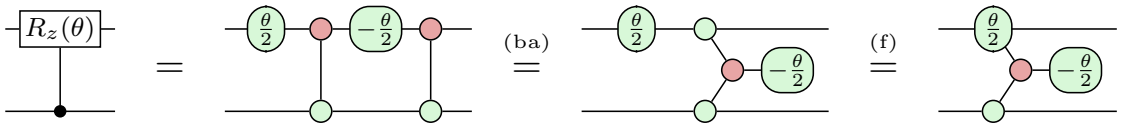

Singly-controlled X and Y rotations obtained by conjugating the control qubit.

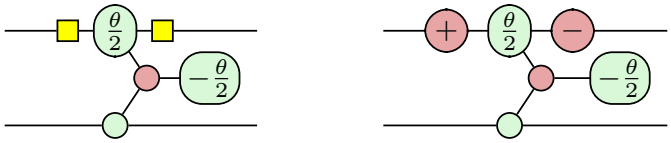

6.2 Doubly-Controlled Rotations

6.3 Triply-Controlled Rotations

Chapter 7

Conclusion

7.1 Conclusion

7.2 Future Work

Appendices

Bibliography

[1] Burton, H. G. A., Marti-Dafcik, D., Tew, D. P. & Wales, D. J. Exact electronic states with shallow quantum circuits from global optimisation. *npj Quantum Information* **9** (2023).

[2] Yeung, R. Diagrammatic design and study of ansätze for quantum machine learning (2020). 2011.11073.

[3] McClean, J. R., Romero, J., Babbush, R. & Aspuru-Guzik, A. The theory of variational hybrid quantum-classical algorithms. *New Journal of Physics* **18**, 023023 (2016).

[4] Kirby, W. M. & Love, P. J. Variational quantum eigensolvers for sparse hamiltonians. *Phys. Rev. Lett. 127, 110503 (2021)* **127**, 110503 (2020). 2012.07171.

[5] Nielsen, M. A. & Chuang, I. L. *Quantum Computation and Quantum Information: 10th Anniversary Edition* (Cambridge University Press, 2012).

[6] Szabó, A. v. & Ostlund, N. S. *Modern quantum chemistry : introduction to advanced electronic structure theory* (Mineola (N.Y.) : Dover publications, 1996). URL http://lib.ugent.be/catalog/rug01:000906565.

[7] Helgaker, T., Jørgensen, P. & Olsen, J. *Molecular Electronic-Structure Theory* (Wiley, 2000).

[8] Fetter, A. L., Walecka, J. D. & Kadanoff, L. P. *Quantum Theory of Many Particle Systems*, vol. 25 (AIP Publishing, 1972).

[9] Anand, A. *et al.* A quantum computing view on unitary coupled cluster theory. *Chemical Society Reviews* **51**, 1659–1684 (2021). 2109.15176.

[10] Chan, H. H. S., Fitzpatrick, N., Segarra-Martí, J., Bearpark, M. J. & Tew, D. P. Molecular excited state calculations with adaptive wavefunctions on a quantum eigensolver emulation: reducing circuit depth and separating spin states. *Physical Chemistry Chemical Physics* **23**, 26438–26450 (2021).

[11] Seeley, J. T., Richard, M. J. & Love, P. J. The bravyi-kitaev transformation for quantum computation of electronic structure. *The Journal of Chemical Physics* **137** (2012). 1208.5986.

[12] Peruzzo, A. *et al.* A variational eigenvalue solver on a photonic quantum processor. *Nature Communications* **5** (2014).

[13] Evangelista, F. A., Chan, G. K.-L. & Scuseria, G. E. Exact parameterization of fermionic wave functions via unitary coupled cluster theory. *The Journal of Chemical Physics* **151** (2019). 1910.10130.

[14] van de Wetering, J. Zx-calculus for the working quantum computer scientist (2020). 2012.13966.

[15] Kissinger, A. & van de Wetering, J. Pyzx: Large scale automated diagrammatic reasoning. *Electronic Proceedings in Theoretical Computer Science* **318**, 229–241 (2020).

[16] Gidney, C. Stim: a fast stabilizer circuit simulator. *Quantum* **5**, 497 (2021).